ISBN: 978-3-95450-249-3 ISSN: 2673-5350 doi: 10.18429/JACoW-IBIC2024-WEP10

OPTIMIZED DESIGN OF AN CONSECUTIVE DOUBLE-SLIT EMITTANCEMETER FOR THE C-BAND PHOTOCATHODE RF GUN*

W. Chen, S. Jiang, R. Liu, T. Yang, R. Yang†, X. Li, S. Wang
Institute of High Energy Physics, 100049 Beijing, China
also at China Spallation Neutron Source, Dongguan, China
X. Li, Deutsches Elektronen-Synchrotron, Zeuthen, Germany

Abstract

To enhance the performance of the next generation of X-ray free electron lasers (XFEL), it is essential to produce a high quality electron beam with a low emittance, for instance, below 0.2 mm-mrad for a 100 pC bunch charge. In order to demonstrate the fundamental techniques required for future FEL facilities, a C-band photoinjector test facility has been constructed aligning with the Southern Advanced Photon Source (SAPS) pre-research project. An emittancemeter based on the consecutive double-slit-scan concept has been proposed and designed for determining such small emittance. This paper presents the further optimization of the primary parameters of this emittancemeter employing numerical simulations in the presence of the measured motion accuracy and the expected observation resolution.

INTRODUCTION

Next-generation XFEL is rapidly moving towards providing more flexible photon pulse time patterns and higher average brightness. This has brought new requirements on the high-brightness electron source to deliver the electron beam with a low transverse normalized emittance (below 0.2 mm-mrad for a bunch charge of 100 pC). High-brightness photocathode electron gun plays a decisive role in the overall performance of XFEL. Among the brightest electron sources, the photoinjector equipped with a low-intrinsic-emittance photocathode has been widely used. For a photocathode radio-frequency gun (RF gun), the beam emittance usually reaches its minimum for an acceleration gradient of about 140-150 MV/m [1, 2]. However, the existing L-band and S-band photocathode RF gun could hardly reach such high acceleration gradient. The C-band photocathode RF gun features a maximum gradient of above 150 MV/m and can provide small-emittance beam for the future XFEL. Moreover, the C-band RF gun has a reasonable requirement on the mechanical processing accuracy (about 20 μm) that could be met with the state-of-art techniques.

The C-band photoinjector test facility at the Institute of High Energy Physics (IHEP/CAS) employs a 5.712 GHz 3.6-cell gun with the designed acceleration gradient above 150 MV/m [3]. To optimize the beam emittance, the beam tracking software Astra combined with Python's lume-astra and Geatpy libraries have been used. An evolutionary algorithm has optimized the minimum emittance at a distance of 1 m from the cathode surface as summarized in Table 1. The cathode material is copper, and the beam energy at the electron gun exit is 7-8 MeV. For a bunch charge of 100 pC, the 100 % and 95 % emittances are 0.18 and 0.11 mm-mrad, respectively. To quantify the beam quality at the gun exit, a diagnostic beamline has been designed. It consists of an emittancemeter (EM), an integral beam transformer (ICT), two screen monitors and a Faraday cup (FC), as shown in Fig. 1.

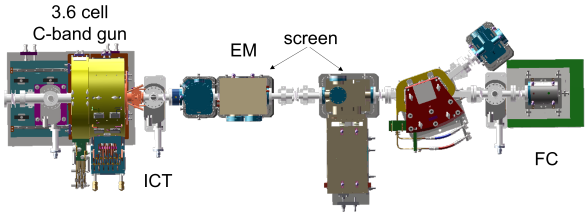

Figure 1: Layout of the C-band photocathode RF gun test facility.

Table 1: Optimum Simulated Photoinjector Parameters for Bunch Charge 100 pc

Parameter	Unit	Value
RF frequency	GHz	5.712
Accelerating gradient	MV/m	150
Repetition rate	Hz	1-100
Beam energy at the gun exit	MeV	7.3
Transverse emittance	mm-mrad	0.175
Bunch length	ps	5
Beam rms size	μm	42.5

METHODS

For the C-band photoinjector, beam emittance increases rapidly from 0.18 mm-mrad to about 0.8 mm-mrad as the beam drifts from a distance of 1 m to 1.8 m. The conventional quadrupole scan and multi-screen method could not be adapted. Alternatively, the multi-slit method or single-slit methods have been widely used at many photoinjector [4–7]. For instance, PITZ measured an emittance of 0.26 mm-mrad employing a 10 μm slit [8]. The both methods employ a tight slit to divide the beam into smaller beamlets and then visualize the beamlet downstream using a profile monitor. Thus, it allows the reconstruction of the phase space distribution and emittance with an acceptable impact from the space-charge effect. The multi-slit method has the merit of single-shot

* GUANGDONG BASIC AND APPLIED BASIC RESEARCH FOUNDATION (2022A1515140179).
† yangrenjun@ihep.ac.cn

ISBN: 978-3-95450-249-3 ISSN: 2673-5350 doi: 10.18429/JACoW-IBIC2024-WEP10

emittance measurement. However, one must avoid or correct the overlap between beamlets. Meanwhile, the single-slit method could reconstruct the almost full phase-space distribution at the cost of a long scan time. But, the systematic evaluation of the measurement accuracy and error are still of great importance.

Single Slit Method

To characterize the influence of the space charge force on the beam, the envelope equation for the relativistic electron beam in free space under the paraxial approximation could be expressed as [9]

$$\sigma_x'' - \frac{{\varepsilon_n}^2}{\gamma^2\sigma_x^3} - \frac{4I_A}{\gamma^3\beta^3 I_0(\sigma_x+\sigma_y)} = 0, \tag{1}$$

where I_A is peak current of beam, I_0=17 kA the electron's Alfven current, ε_n the normalized emittance, σ_x, σ_y the transverse root mean square (rms) beam sizes, γ the Lorentz factor, β the electron velocity scaled by light speed. Typically, we use the space-charge dominance ratio R_{sc} to quantify the degree of space-charge dominance over emittance in driving the evolution of the beam envelope. The R_{sc} is defined by the ratio of the second and third terms in Eq. (1). To mitigate the space-charge force, R_{sc} should be much smaller than 1. As suggested in Ref. [10], One may consider that the beam is emittance-dominated when R_{sc} is smaller than 0.1.

Concerning the design beam parameters at the exit of the C-band photocathode RF gun, R_{sc} is about 2.5, i.e., the beam is space charge dominated. For the beamlet at the slit exit, the beamlet width can be approximated as $w/\sqrt{12}$ where w is slit width. The space-charge dominance ratio could be then approximated as

$$R_{sc} = \frac{4Iw^2}{5\sqrt{3}\gamma\beta^3 I_0\varepsilon_n^2(1+w/\sqrt{12}\sigma_x)}, \tag{2}$$

where I the beamlet peak current which could be approximated as [11]

$$I = I_A w/2.5\sigma_x. \tag{3}$$

Apparently, a narrow slit to divide the beam into more smaller beamlets could effectively reduce the space charge force and its influence. For the beam parameters at the gun exit at a bunch charge of 100 pC, the preliminary evaluation by Eq. (2) reveals that a slit width of less than 9.1 µm is necessary to ensure the emittance dominance of the beamlet (R_{sc} = 0.1).

Consecutive Double-Slit Method

We have proposed an emittance measurement technique based on the consecutive double-slit-scan concept. By using a second slit parallel to the first slit, one can divide the beamlet into sub-beamlets. Thus, it is possible to further mitigate the measurement error arising from the space charge force, as depicted in Fig. 2.

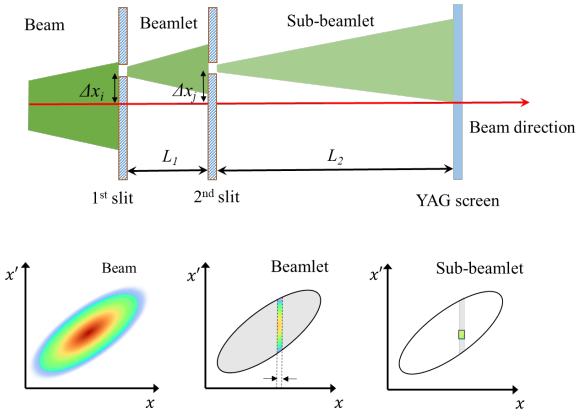

Figure 2: The illustration of the consecutive double-slit scheme.

Knowing the slit position and the sub-beamlet distributions, one can reconstruct the distribution and the rms divergence of the beamlet as

$$\begin{aligned} x'_i &= \frac{\sum_{j=1}^{m} x_{i,j} - \Delta x_i}{L_1+L_2} \\ \sigma'_i &= \frac{\sigma_i}{L_1+L_2} \end{aligned}, \tag{4}$$

where $x_{i,j}$ is the position distribution of the j-th sub-beamlet after the i-th beamlet passes through the second slit, m is the total number of the sub-beamlets derived from a single beamlet, Δx_i is the central position of the first slit corresponding to the i-th beamlet, σ_i is the rms size of the accumulation of sub-beamlets profile from i-th beamlet. L_1 and L_2 are the drift length of the beamlet from the first slit to the second slit and the drift length of the sub-beamlets from the second slit to the screen, respectively. Then, the first moments of the phase-space distribution could be approximated as

$$\begin{aligned} \langle x\rangle &= \frac{\sum_{i=1}^{n} I_i x_i}{\sum_{i=1}^{n} I_i} \approx \frac{\sum_{i=1}^{n} I_i \Delta x_i}{\sum_{i=1}^{n} I_i} \\ \langle x'\rangle &= \frac{\sum_{i=1}^{n} I_i x'_i}{\sum_{i=1}^{n} I_i} \end{aligned}, \tag{5}$$

where I_i is the integrated detected intensity of the i-th beamlet, n the total number of beamlets, x_i the distribution of the ith beamlet. The second moments of the phase-space distribution and the emittance could be expressed as

$$\begin{aligned} \langle x^2\rangle &= \frac{\sum_{i=1}^{n} I_i(\Delta x_i - \bar{x})^2}{\sum_{i=1}^{n} I_i} \\ \langle x'^2\rangle &= \frac{\sum_{i=1}^{n} I_i\left[(x'^2 - \bar{x}')^2 + \sigma'^2{}_i\right]}{\sum_{i=1}^{n} I_i} \\ \langle xx'\rangle &= \frac{\sum_{i=1}^{n} I_i(\Delta x_i - \bar{x})(x'^2 - \bar{x}')}{\sum_{i=1}^{n} I_i} \\ \varepsilon_n &= \gamma\beta\sqrt{\langle x^2\rangle\langle x'^2\rangle - \langle xx'\rangle^2} \end{aligned}, \tag{6}$$

where $\bar{x}$ and $\bar{x}'$ are the mean position and the mean divergence of entire beam, respectively.

ISBN: 978-3-95450-249-3 ISSN: 2673-5350 doi: 10.18429/JACoW-IBIC2024-WEP10

The measurement accuracy also depends on the algorithm of emittance analysis. Due to a limited signal-to-noise ratio (SNR), an imperfect image noise subtraction and a weak signal recognition, it's impossible to reconstruct the 100 % of the emittance. Thus, a more appropriate measure of the result is the 95 % emittance. The popular emittance evaluation techniques include the threshold method, ellipse exclusion method, and single projection ellipse analysis (SPEA) [12]. Hereinafter, the SPEA method is used to fit the reconstructed phase space distribution and determine the 95 % emittance.

EMITTANCEMETER DESIGN

The primary parameters of an emittancemeter encompass the slit width, the slit thickness, and the drift distance [13–16]. Compared with traditional single-slit method, the consecutive double-slit method has another key parameter L_1. The concept design of the emittancemeter in Ref. [17] emphasises on the control of the central-beamlet size. However, to reduce the measurement error, the optimization of the emittancemeter parameters by means of numerical simulation is indispensable.

Preliminary Design

The slit width is important in reducing the space charge force. In order to minimise the space charge force and to ensure reasonable processing accuracy, it is more appropriate to use two 10 µm slits.

The SNR of detection for the downstream sub-beamlets is related to the thickness of the slit mask. The density of sub-beamlets on the downstream observation screen must be higher than the density of both transmitted and scattered particles. Thus, the slit mask must effectively block or deflect the peripheral particles. In order to ensure an acceptable SNR and sensitivity for the emittance measurement, a tungsten slit mask with a thickness of 1 mm was selected regarding the Monte Carlo simulations and the fabrication difficulties [18].

If the drift distance L_1 is insufficient, the beamlet cannot be divided into the smaller sub-beamlets with lower bunch charge before fully diverging. Conversely, when L_1 is excessive, the beamlet distribution was more significantly altered by the more potent space charge force before reaching the latter slit. In this case, the performance of this emittancemeter will be similar to that employing a single-slit of the same slit width. Assuming a total drift distance of 0.55 m, the optimized of the beamlet's drift distance concerning the measurement error is considered. To obtain a measurement error below 8 %, L_1 should be within 0.03-0.04 m, as shown in Fig. 3.

An appropriate drift distance of the sub-beamlet is also necessary for measurement accuracy. As shown in Fig. 4, for a drift distance of 0.26 m, the measurement error could be minimized to about 5 % and the L_1 parameter at 0.04 m. It is also observed that the increase of the measurement error caused by space charge force is quantified to be less than 1 % when the drift distance is from 0.26 m to 0.5 m. After being further attenuated by the second slit, the sub-beamlet is emittance dominant when the drift distance is sufficiently large.

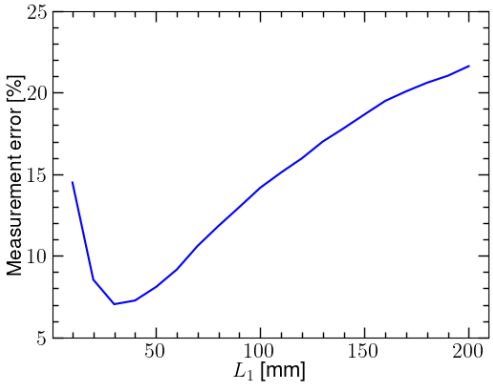

Figure 3: Measurement error versus the distance of two slits L_1.

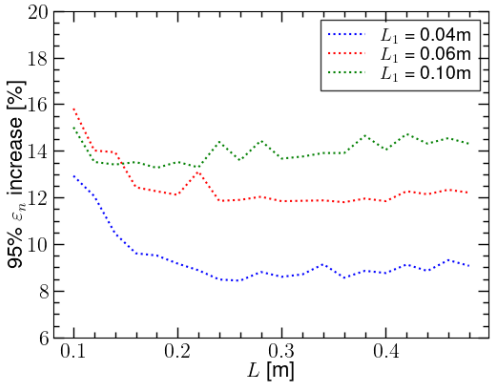

Figure 4: Measurement error versus L_2 when L_1 at 0.01, 0.06, 0.10 m.

Dynamic Errors and Their Impacts

In addition to the space charge force, the accuracy of the emittance measurement is mainly determined by dynamic errors, e.g., the displacement accuracy of the linear stage and the image resolution of the beamlet or sub-beamlet profile. Typically, the slit scan is driven by a motor equipped with a grating ruler. The off-line measurements using a laser tracker has indicated a rms displacement accuracy of about 0.8 µm for an unidirectional scan with a step size of 10 µm.

For a beam size of 10-100 µm, a YAG screen has been considered to imagine the sub-beamlet distribution. The screen is perpendicular to the beam trajectory, and the fluorescence light is transported in to the in-air optical observation system through a mirror in downstream. Concerning Optical diffraction limit, optical aberrations, YAG screen thickness and sensor pixel size, the resolution of our image system has been assessed as less than 10 µm.

Based on the above evaluations, the drift distances L_1 and L_2 have been further optimized. Considering the dynamic errors, the optimal drift distance of sub-beamlet is about 0.24 m with a minimum measurement error of 7.3 %,

ISBN: 978-3-95450-249-3 ISSN: 2673-5350 doi: 10.18429/JACoW-IBIC2024-WEP10

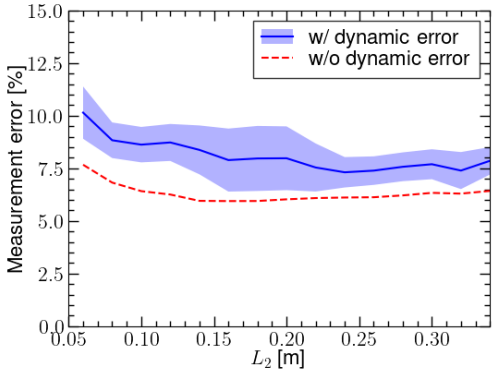

Figure 5: Measurement error versus L_2.

as shown Fig. 5. Compared to the preliminary design in the above sub-section, the dynamic error enlarges the reconstructed beam divergence and the drift distance of sub-beamlet should be longer.

By optimizing the drift distance, the parameters of the emittancemeter are essentially established, which allows the assessment of the measurement errors. We have re-optimized the drift distances for single-slit scan with slit widths of 5 µm and 10 µm, and consecutive double-slit scan with two 10 µm slits. As shown in Fig. 6 (a), the single-slit scan with a slit width of 5 µm and 10 µm has a minimum measurement error of 4.7 % and 14 %, respectively. Meanwhile, the consecutive double-slit scan can minimize the measurement error to about 7.3 %, as shown in Fig. 6 (b).

The Scope of Applications

In order to determine the applicability domain of the consecutive double-slit method, the phase space distribution of the beam with bunch charge 100 pC is manipulated to produce a variety of emittances from 0.1 to 0.3 mm.mard. For a smaller emittance, the mitigation of space-charge force is weakened accompanied with a higher beam loss. But, it is possible to diagnose higher beam emittances with smaller impact of space charge force. For an emittance of 0.1-0.15 mm-mrad, the measurement error of consecutive double-slit scan exceeds 10 %. For an emittance of 0.15-0.25 mm-mrad, the measurement error of consecutive double-slit scan remains below 10 %, whereas the measurement error of single-slit scan is over 10 %, as shown in Fig. 7. Moreover, the consecutive double-slit scan, which uses one of the two slits, can measure an emittance of over 0.26 mm·mrad with a measurement error below 10 %.

CONCLUSION

To quantify the beam emittance from a C-band photocathode RF gun with a acceptable accuracy, a consecutive double-slit emittancemeter has been proposed. In the presence of the expected dynamic errors, the slit width, slit thickness and the drift distances have been optimized. Concerning the beam parameters at a bunch charge of 100 pC, a minimum measurement error of 7.3 % has been predicted for a slit width of 10 µm, a slit thickness of 1 mm, a beamlet

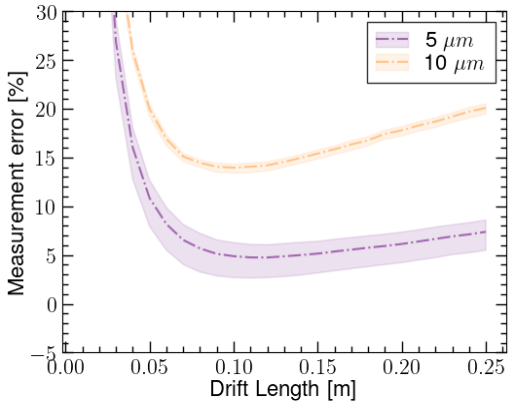

(a) single-slit scan

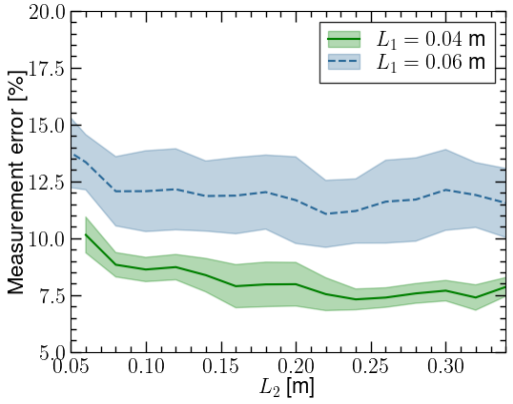

(b) consecutive double-slit scan

Figure 6: Optimized the drift distance for a single-slit with slit width of 5 and 10 µm (a), and for the consecutive double-slit (b).

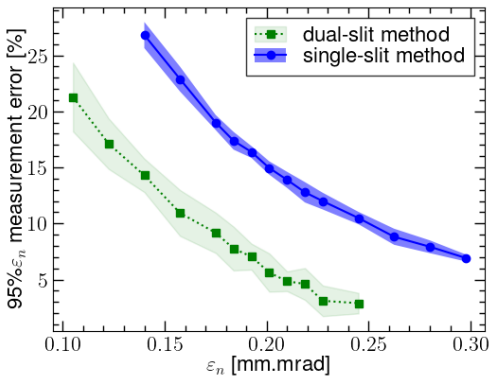

Figure 7: Measurement different emittance error.

drift distance of 0.04 m, and a sub-beamlet drift distance of 0.24 m. Finally, the applicability of the emittancemeter is determined by simulating a range of emittances, specifically measuring emittances over 0.15 mm-mrad with a measurement error of less than 10 %.

ISBN: 978-3-95450-249-3 ISSN: 2673-5350 doi: 10.18429/JACoW-IBIC2024-WEP10

REFERENCES

[1] D. Palmer *et al.*, "Initial commissioning results of the next generation photoinjector", *AIP Conf. Proc.*, vol. 398, pp. 695–704, 1997. doi:10.1063/1.53071

[2] B. Dwersteg *et al.*, "RF gun design for the TESLA VUV free electron laser", *Nucl. Instrum. Methods Phys. Res., Sect. A*, vol. 393, pp. 93–95, 1997. doi:10.1016/S0168-9002(97)00434-8

[3] X. Liu *et al.*, "A C-band test platform for the development of RF photocathode and high gradient accelerating structures", in *Proc. IPAC2023*, Venice, Italy, May 2023, pp. 1995-1998. doi:10.1088/1742-6596/2687/4/042001

[4] C. Liu *et al.*, "Multi-slit emittance measurement study for BNL ERL", BNL, Upton, NY, USA, Rep. BNL-98657-2012-IR, Oct. 2012. doi:10.2172/1054184

[5] M. Zhang *et al.*, "Emittance formula for slits and pepper-pot measurement", Fermi National Accelerator Laboratory, IL, USA, Rep. FNAL-TM-1988, Oct. 1996.

[6] M. Minty *et al.*, *Measurement and Control of Charged Particle Beams*. Heidelberg: Springer Berlin, 2003, pp. 99–111. doi:10.1007/978-3-662-08581-3

[7] P. Forck *et al.*, "Lecture Notes on Beam Instrumentation and Diagnostics", presented at the Joint University Accelerator School, Darmstadt, Germany, Jan.–Mar. 2011, pp. 65-77.

[8] H. Qian *et al.*, "Analysis of photoinjector transverse phase space in action and phase coordinates", *Phys. Rev. Accel. Beams*, vol. 25, p. 103401, Oct. 2022. doi:10.1103/PhysRevAccelBeams.25.103401

[9] R. Martin *et al.*, *Theory and Design of Charged Particle Beams*. Wiley-VCH Verlag GmbH & Co. KGaA, 2008, pp. 180–181. doi:10.1002/9783527622047

[10] L. Staykov, "Design Optimization of an Emittance Measurement System at PITZ", in *Proc. DIPAC'05*, Lyon, France, Jun. 2005, paper POT032, pp. 220–222.

[11] T. Tao *et al.*, "Sub-Micron Normalized Emittance Measurement for a MeV Continuous-Wave Electron Gun", *Nucl. Instrum. Methods Phys. Res., Sect. A*, vol. 1045, p. 167552, 2023. doi:10.1016/j.nima.2022.167552

[12] A. Mostacci *et al.*, "Analysis Methodology of Movable Emittance-Meter Measurements for Low Energy Electron Beams", *Rev. Sci. Instrum.*, vol. 79, no. 1, p. 013303, 2008. doi:10.1063/1.2835715

[13] K. Togawa *et al.*, "CeB6 electron gun for low-emittance injector", *Phys. Rev. ST Accel. Beams*, vol. 10, p. 020703, 2007. doi:10.1103/PhysRevSTAB.10.020703

[14] L. Yan *et al.*, "Multislit-Based Emittance Measurement of Electron Beam from a Photocathode Radio-Frequency Gun", *Chin. Phys, Lett.*, vol. 25, pp. 1640–1643, 2008. doi:10.1088/0256-307X/25/5/032

[15] C. Liu *et al.*, "Transverse Beam Emittance Measurements with Multi-Slit and Moving-Slit Devices for LEReC", in *Proc. IBIC2018*, Shanghai, China, Aug. 2018, pp. 486–489. doi:10.18429/JACoW-IBIC2018-WEPB21

[16] R. Niemczyk *et al.*, "Slit-Based Slice Emittance Measurements Optimization at PITZ", in *Proc. IBIC2019*, Malmö, Sweden, Sep. 2019, pp. 318–321. doi:10.18429/JACoW-IBIC2019-TUPP013

[17] R. Yang *et al.*, "A consecutive double-slit emittance meter for high-brightness electron source", in *Proc. IPAC2023*, Venice, Italy, Mar. 2023, pp. 4721–4724. doi:10.18429/JACoW-IPAC2023-THPL110

[18] S. G. ANDERSON *et al.*, "Space-charge effects in high brightness electron beam emittance measurements", *Phys. Rev. ST Accel. Beams*, vol. 5, p. 014201, 2002. doi:10.1103/PhysRevSTAB.5.014201